

On the threshold of motion of sediment grains: Hydrodynamic forces effects

Reza Barati and Seyed Ali Akbar Salehi Neyshabouri
Faculty of Civil and Environmental Engineering
Tarbiat Modares University
Tehran, Iran
r88barati@gmail.com; salehi@modares.ac.ir

Goodarz Ahmadi
Department of Mechanical and Aeronautical Engineering
Clarkson University
Potsdam, New York, USA
gahmadi@clarkson.edu

Abstract—Particle movement will occur when the instantaneous fluid force on a particle is just larger than the instantaneous resisting force. One of the most important issues in this regard is the influence of different hydrodynamic forces on threshold of motion. In the present study, effects of different forces; such as non-linear drag force, the shear lift force, Magnus force, the buoyancy force, the added mass force, Basset history force and torque; on the initiation of motion of sediment grains were studied by developing a 3D Lagrangian numerical model. The particle-wall collision were included using Discrete Element Method (DEM) and a random process. The non-cohesive sediments grains for the range of sand to gravel were considered. The verification step was performed using different particle diameters and flow conditions. The results indicated that the drag force is the dominating force. Also, it is observed that the influence of lift force increase by increasing grain diameter.

Keywords: Numerical modeling, Sediment transport, Incipient motion, forces.

I. INTRODUCTION

A sediment grain at the bed surface of alluvial streams is subject to hydrodynamic forces. When the flow velocity increases, the magnitudes of hydrodynamic forces increase, and sediment grains begin to move if the hydrodynamic forces go beyond a critical value which is commonly called **incipient motion** or **threshold of motion** [1]. The investigation of the threshold conditions is an important issue because it can be used to discover the fundamental mechanism of the sediment transport.

There are several approaches for the estimation of the critical conditions of the sediment movement such as critical mean velocity, critical bed shear stress, critical stream power and critical water discharge [2]. However, the common procedure is Shields diagram [3] which is based on the estimation of dimensionless critical shear stress $\tau_c^* = \tau_c / [(\gamma_s - \gamma)d]$ as function of the particle Reynolds number $R_* = u_c^* d / \nu$, where τ_c is the critical shear stress for onset of incipient motion, γ_s is the specific weight of the sediment grain, γ is the specific weight of the water, d is the particle diameter, u_c^* is the critical shear velocity and ν is the

kinematic viscosity. Such approach can be used to estimate the critical condition in a deterministic manner, whereas the phenomenon is naturally stochastic because of the fluctuations of the turbulent flow and the bed roughness. This issue is addressed in Figure 1 by collecting available experimental data of the threshold of motion of the sediment grains in terms of Shields parameter (i.e. dimensionless critical shear stress) (please see [4] for more details of experimental data). It should be noted that the difference in incipient motion definitions is the one of the sources of the scatter in experimental results as well as aforementioned factors. The visual observation, reference transport method, largest grain method, and probabilistic approach are some common methods of defining threshold of motion [2].

The use of Newton's second law is an effective approach for taking to account different hydrodynamic forces which exert on the sediment grains by considering Lagrangian–Eulerian modeling. Dozens of the application of such approach for the simulation of the particles movement in air and water have been published in the literature (e.g. [5], [6], [7], [8], [9], [10], [11], [12], [13], and [14]). However, among sediment transport studies, most of them were focused on the saltation motion.

One of the most important issues in the sediment transport engineering is the contribution of each force on the incipient motion. The present study aims to analyze the effects of the different hydrodynamic forces on the initial movement of the sediment grains. To elaborate the problem, a 3D Lagrangian–Eulerian model was developed by considering various hydrodynamic forces including non-linear drag force, the shear lift force, Magnus force, the buoyancy force, the added mass force, Basset history force and torque. The logarithmic law was used for the mean flow velocity in the longitudinal direction. In order to reflect the stochastic nature of the phenomenon, a nondeterministic particle-bed collision model was adopted. The developed model was *validated* against experimental data previously for the bed-load transport in the saltation regime [15] and in the incipient motion condition [16]. Therefore, it can be utilized as a tool for the numerical experiment of the sediment transport.

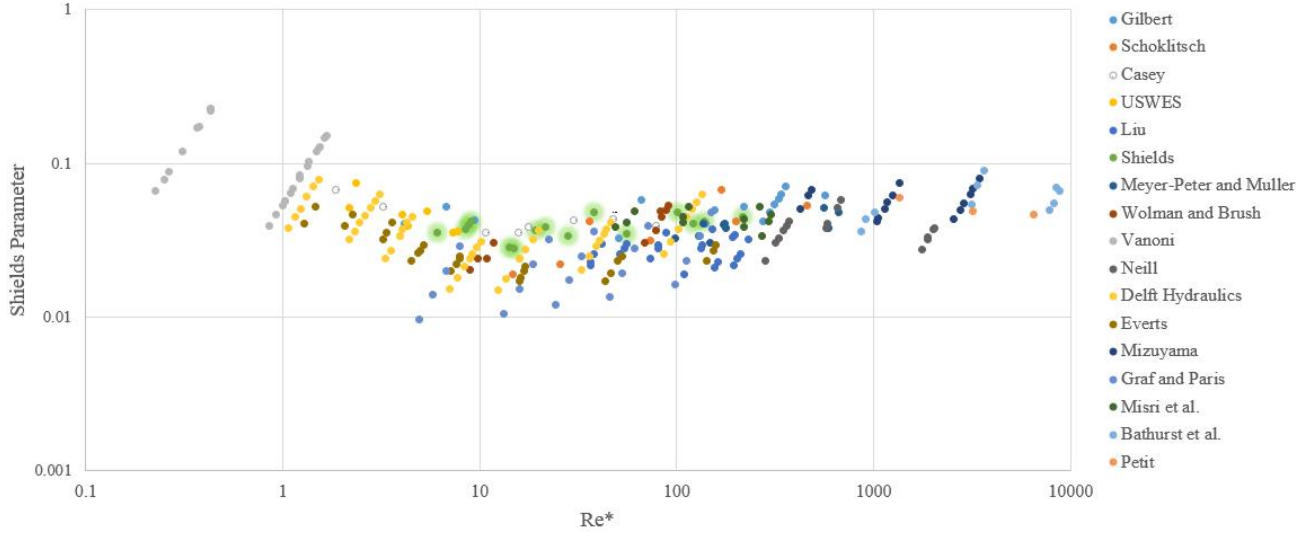


Figure 1. The presentation of the stochastic nature of the incipient motion of the sediment grains

II. MODEL DESCRIPTION

A. Governing equation of the particle movement

A particle tracking model which can describe the location of each particle at each time step needs for the representation the two-phase flow in the Eulerian-Lagrangian modeling [17]. The Newton's second law can be used to calculate the position, velocity, and acceleration of the particles by considering the hydrodynamic forces acting on each particle.

For a small spherical particle in an unbounded fluid, Maxey and Riley [18] presented a linear moment equation within the Stokes drag range (i.e. MR equation). However, for the sediment transport some changes must be performed. Therefore, the governing equations were improved over the time by various researchers for the sediment transport in water. In this regard, Wiberg and Smith [19] developed a theoretical model. Nino [6] adopted MR equation with the conditions of the movement of the sediment in water. However, the studies were not used the angular moment equation for taking to account the particle rotation, effectively. Some other studies (for example Gonzalez [17]) used such equation for the modeling.

An optimal model framework were adopted in the present study as:

$$\frac{d\bar{x}_p}{dt} = \bar{u}_p \quad (1)$$

$$m_p \frac{d\bar{u}_p}{dt} = F_{AM} + F_D + F_L + F_M + F_B + F_G \quad (2)$$

$$I_p \frac{d\bar{\omega}_p}{dt} = \bar{T} \quad (3)$$

where \bar{x}_p the particle position vector, \bar{u}_p is the particle velocity vector, t is the simulation time, m_p is the particle

mass, F_{AM} is the added mass force, F_D is the drag force, F_L is the shear lift force, F_M is the Magnus force, F_B is the Basset history force, F_G is the buoyancy force, $I_p=0.1m_pD^2$ is the particle moment of inertia, $\bar{\omega}_p$ is angular velocity of the

grain and \bar{T} is the torque vector acting on the particle. The details of the hydrodynamic forces were described in [15].

It should be stated some coefficients of the hydrodynamic forces such as nonlinear drag was improved in the model [20] and [21].

B. Fluid flow model

The Navier–Stokes equations are the governing equations of fluid flow. However, some experimental studies showed that a logarithmic distribution for the mean flow velocity is valid for bed-load sediment transport from low to medium flow tractive forces [22]. The following logarithmic profile was implemented in the present model:

$$\frac{\bar{u}_f(y)}{u^*} = \frac{1}{\kappa} \ln\left(\frac{y}{K_s}\right) + B \quad (4)$$

where u^* is the shear velocity, y is the distance from the bed, $\kappa=0.41$ is the von Karman constant, K_s is the effective roughness of the bed and $B=8.5$ is a constant.

C. Particle-bed collision model

To simulate the continuous motion of a sediment grain in water, a collision model must be applied. Such a model has two main parts including a series of equations to describe the grain velocity after the rebound and a bed roughness model. The later part is more important than the first one. The most common approach is Nino [6] model which is based on the relation between three angles associated with particle-bed collision. However, this model do not take into account grain rotation after particle-bed collision.

In the present study, a particle-bed collision model based on the impulse equations is adopted [5]. For the representation of the bed roughness, the concept of the contact zone was used to consider the irregularity of the bed [10]. In this approach, two random angles were used to select a contact point in the possible contact zone, and then four consecutive coordinate transformations were performed to reach the translational and angular velocities in the contact coordinate. The velocities after the collision can be calculated using discrete element method depending on whether the particle slides or not on the bed. A particle slides if the following expression is satisfied:

$$\frac{u_y^{(0)}}{|V|} < -\frac{2}{7f(e+1)} \quad (5)$$

If the criterion is met, the stream-wise, the span-wise and wall-normal directions of the translational velocities are calculated as:

$$u_x = \frac{5}{7} \left(u_x^{(0)} - \frac{d}{5} \omega_z^{(0)} \right) \quad (6)$$

$$u_y = -eu_y^{(0)} \quad (7)$$

$$u_z = \frac{5}{7} \left(u_z^{(0)} + \frac{d}{5} \omega_x^{(0)} \right) \quad (8)$$

And angular velocities are calculated as:

$$\omega_x = 2v_z/d \quad (9)$$

$$\omega_y = \omega_y^{(0)} \quad (10)$$

$$\omega_z = -2v_x/d \quad (11)$$

If the particle does not slide the post-collision translational and angular velocities are calculated as:

$$u_x = u_x^{(0)} + \varepsilon_x f (e+1) u_y^{(0)} \quad (12)$$

$$u_z = u_z^{(0)} + \varepsilon_z f (e+1) u_y^{(0)} \quad (13)$$

$$u_z = u_z^{(0)} + \varepsilon_z f (e+1) u_y^{(0)} \quad (14)$$

$$\omega_x = \omega_x^{(0)} - \frac{5}{d} \varepsilon_z f (e+1) u_y^{(0)} \quad (15)$$

$$\omega_z = \omega_z^{(0)} + \frac{5}{d} \varepsilon_x f (e+1) u_y^{(0)} \quad (16)$$

$$\omega_z = \omega_z^{(0)} + \frac{5}{d} \varepsilon_x f (e+1) u_y^{(0)} \quad (17)$$

where f is the friction coefficient, e is the coefficient of restitution, $(u_x^{(0)}, u_y^{(0)}, u_z^{(0)})$ and (u_x, u_y, u_z) denote, respectively, translational velocities before and after collision in stream-wise, wall-normal and span-wise directions, $(\omega_x^{(0)}, \omega_y^{(0)}, \omega_z^{(0)})$ and $(\omega_x, \omega_y, \omega_z)$ are the

corresponding angular velocities,

$$|V| = \sqrt{(u_x^{(0)} + 0.5d \omega_z^{(0)})^2 + (u_z^{(0)} - 0.5d \omega_x^{(0)})^2}$$

$$\varepsilon_x = (u_x^{(0)} + 0.5d \omega_z^{(0)})/|V| \text{ and } \varepsilon_z = (u_z^{(0)} - 0.5d \omega_x^{(0)})/|V|.$$

Backward transformations of the above calculated velocity vectors to the original coordinate system will be performed.

D. Final developed model

The system of governing equations [i.e. Eqs. (1) to (3)] is numerically solved using either the fourth-order Runge-Kutta method or Runge-Kutta-Fehlberg method if appropriate initial conditions are considered. In order to investigate the incipient motion of the sediment grains, all of the initial translational and angular velocities are set to zero. The initial position of the grain is on the coordinate origin in the horizontal plan while it is placed on $0.5d$ in the wall-normal direction.

The flowchart of the final model is presented in Figure 2. As mentioned in the introduction section, the model was **validated** against experimental data for the **saltation regime** [15] and the **threshold condition** [16] of the bed-load transport in previous studies.

It should be stated that the developed model has a sub-model for particle-particle interaction using DEM. However, it does not presented here because only one moving sediment grain is analysed.

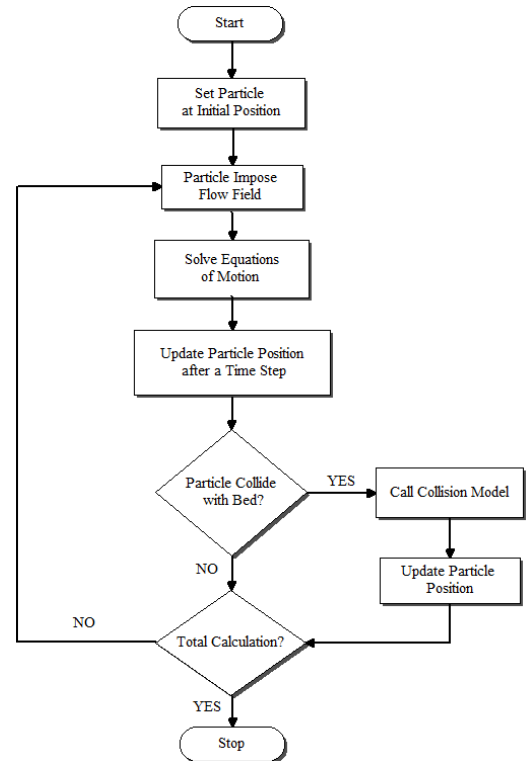


Figure 2. The flowchart of the developed sediment transport model

III. RESULTS AND DISCUSSION

For the analysis of the threshold of motion of the bed-load transport, it is necessary to define such motion. In the present study, the sediment grain is considered in the entrainment condition when it moves one diameter along the longitudinal direction.

The developed model is naturally stochastic because of the presentation of the random bed-particle collision model. Therefore, the model yields different results in consecutive runs with similar inputs. However, the critical shear velocity u_c^* is estimated through a trial and error procedure. The mean value of 100 consecutive runs were considered as u_c^* .

For the illustration of the nondeterministic characteristics of the developed model, the results of ten consecutive runs at the threshold instant for $d=1.5$ cm and $u_c^*=11.5$ cm/s is presented in Figures 3 and 4 in the stream-wise and span-wise directions, respectively. It can be seen that the model

yields different results in different runs while the input parameters of the model is constant.

For the analyses of the effects of the different hydrodynamic forces on the incipient motion instant, the forces (i.e. the drag, shear lift and Magnus forces) become dimensionless with buoyancy force because this force is constant during the movement of the grain. Then, the percentage of the contribution of the each force were calculated.

It should be stated that Lukerchcenko et al [23] concluded that the Basset history force can be neglected when the particle Reynolds number is larger than about 4000 and 8000 for 2D and 3D models, respectively [24]. Therefore, this force can be omitted in the numerical computations, because particle Reynolds number is equal to zero in the incipient motion condition. This issue is illustrated in Figure 5 by representation of the variations of the hydrodynamic forces in stream-wise direction for $d=1.5$ cm and $u_c^*=11.5$ cm/s.

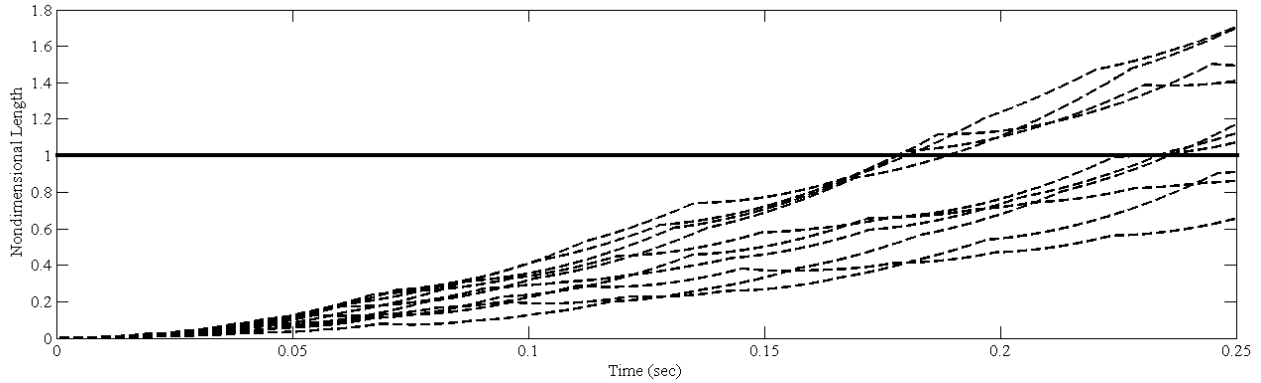


Figure 3. The representation of the stochastic nature of the model at the threshold instant in stream-wise direction

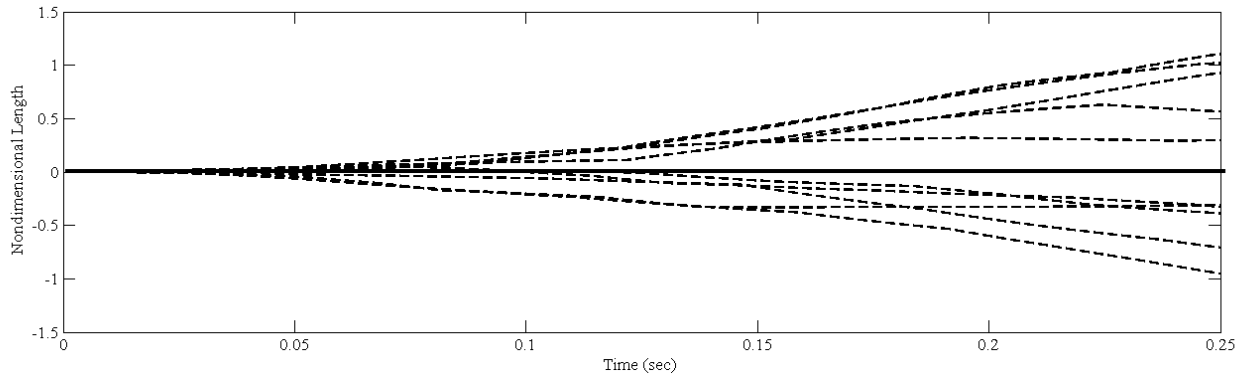


Figure 4. The representation of the stochastic nature of the model at the threshold instant in span-wise direction

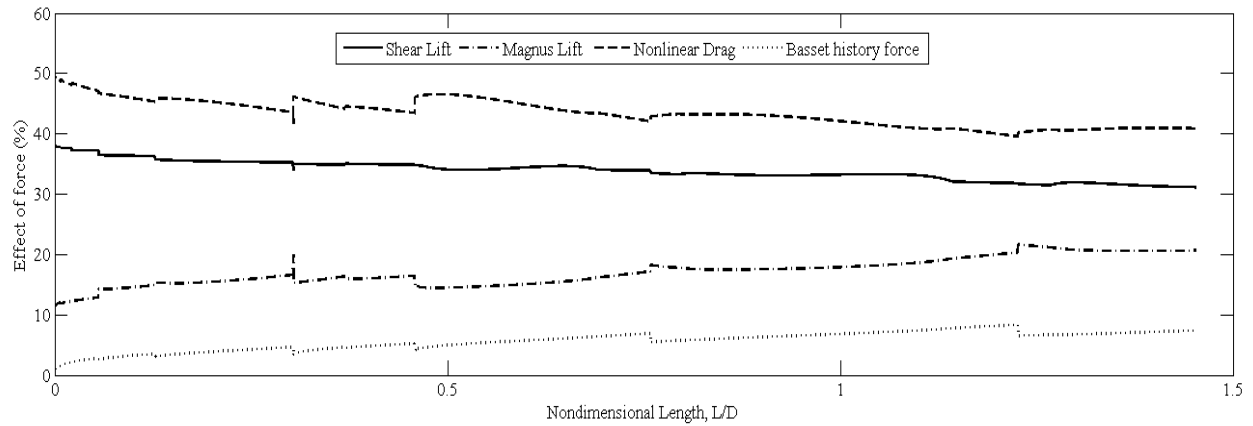


Figure 5. The variations of the hydrodynamic forces in stream-wise direction

It should be noted that the bed roughness of the model is equal to the diameter of the moving grain. Although, this assumption is not important of this analyses, significantly. It can effects of the value of critical shear velocity for the incipient motion of the sediment grains.

Summary of the results is presented in Figures 6 to 8 (for sand grains in Figure 6 and 7 and for gravel grains in Figure 8 and 9). The position of the grain in normal plane (stream-wise and normal directions) as well as the percentage of the contribution of each fore with time were exhibited. Before the discussion the results, it should be stated that the drag, shear lift and Magnus forces are considered in this analyses. Generally, the results indicate that the drag force is the dominating force for sand and gravel grains. However, its contribution varies with increasing grain diameter.

As it can be seen in Figure 6, for a sand grain with diameter 0.05cm, the contribution of the drag force is about 75 %, while the Magnus force is more important than lift force with total contribution about 25%. For a sand grain with diameter 0.1cm (i.e. Figure 7), although the effects of the drag force decreases, its contribution is more than the Magnus and lift forces, and is about 57%.

On the other hand, for a gravel grain with diameter 1.5cm (i.e. Figure 8), the contribution drag force decreases, and reach about 50%. However, the lift force is heir of most of this reduction. In other words, the effects of the lift force is more than Magnus force in the gravel range. Similar trend can be seen by increasing grain diameter from 1.5 to 2.5 cm (see Figure 9).

Interestingly, the previous study (i.e. Barati et al. [15]) which used the developed model for the sediment transport in the saltation regime indicated that shear force is more important than Magnus for the both gravel and sand grains, while the results of the present study indicated that the Magnus force is slightly more important than lift force for the sand grains while the lift force is more important in the gravel grains in the incipient motion conditions.

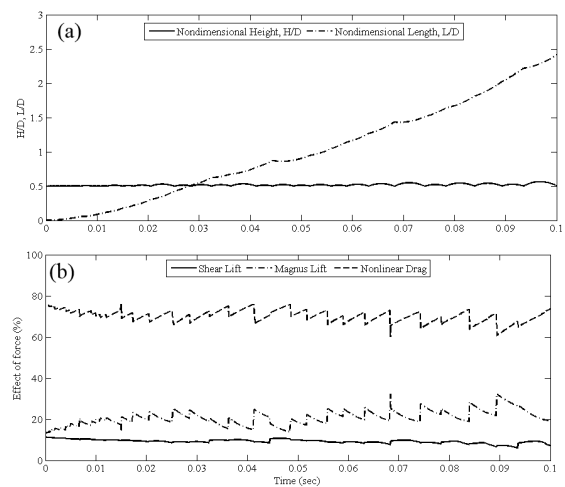


Figure 6. The position of the grain in normal plane (a) and variation of hydrodynamic forces (b) with time for $d=0.05\text{cm}$

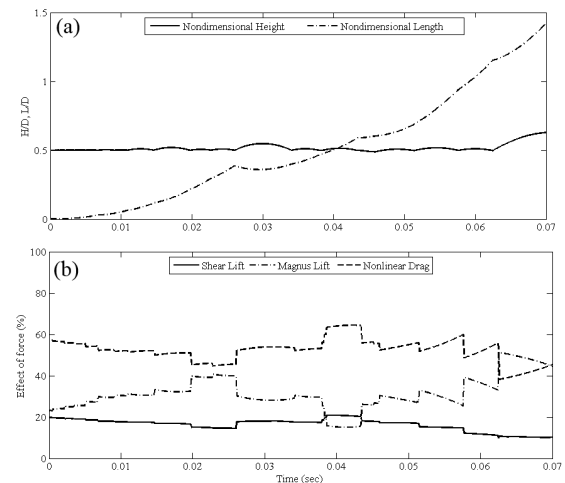


Figure 7. The position of the grain in normal plane (a) and variation of hydrodynamic forces (b) with time for $d=0.1\text{cm}$

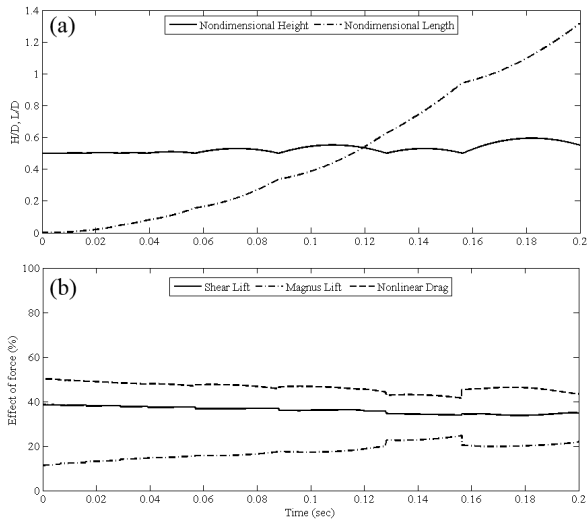


Figure 8. The position of the grain in normal plane (a) and variation of hydrodynamic forces (b) with time for $d=1.5\text{cm}$

IV. CONCLUSIONS

When the flow velocity gradually increases over sediment grains, the grains will start to move if the critical condition satisfies. The investigation of the contribution of the hydrodynamic forces on the initial movement of sediment grains is an important issue in the sediment transport engineering. To elaborate the problem, a 3D Lagrangian–Eulerian model was developed and validated against experimental data for the numerical simulation of noncohesive sediment grains. Various hydrodynamic forces including non-linear drag force, the shear lift force, Magnus force, the buoyancy force, the added mass force, Basset history force and torque were adopted in the model. A stochastic procedure were used for the particle-bed collision model using Discrete Element Method (DEM). The logarithmic law was applied for the mean flow velocity in the longitudinal direction.

One of the most important characteristic of the developed model is the stochastic nature of it. By using such model, the sediment transport modeling which is a random process can be simulated, effectively. Traditionally, the threshold of motion was considered as the shear velocity exceeds a critical value. However, the developed model yields a range of critical values instead of a critical value.

Generally, the results showed that the drag force is the dominate force in both sand and gravel ranges with almost at least half of the total forces (i.e. 50 %). Also, it was observed that the Magnus force is slightly more important than lift force for the sediment grains in sand range while the lift force is more important in the gravel range. Finally, it can be said that the results of the present study indicates the effectiveness of the Lagrangian–Eulerian modeling for the

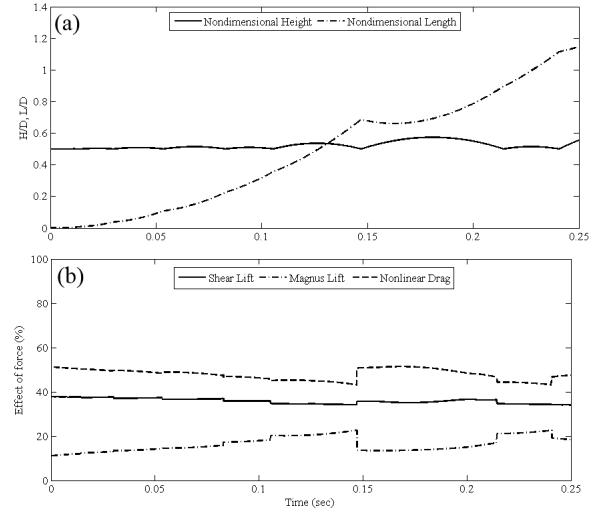


Figure 9. The position of the grain in normal plane (a) and variation of hydrodynamic forces (b) with time for $d=2.5\text{cm}$

investigation of the incipient motion of a sediment grain in various conditions.

REFERENCES

- [1] S. Dey, A.Papanicolaou, "Sediment threshold under stream flow: A state-of-the-art review," *KSCE Journal of Civil Engineering*, Vol.12, No.1, pp. 45-60, 2008.
- [2] A. B. Shvidchenko, "Incipient motion of streambeds," Doctoral dissertation, University of Glasgow, 2000.
- [3] A. Shields, "Application of similarity principles and turbulence research to bed-load movement," *Mitteilungen der Preussischen Versuchsanstalt fur Wasserbau und Schiffbau*, 26, pp. 5-24, 1936.
- [4] J. M. Buffington, D. R. Montgomery, "A systematic analysis of eight decades of incipient motion studies with special reference to gravel-bedded rivers," *Water Resources Research*, Vol.33, No.8, pp. 1993-2029, 1997.
- [5] Y. Tsuji, T. Oshima, Y. Morikawa, "Numerical simulation of pneumatic conveying in a horizontal pipe," *KONA Powder and Particle Journal*, Vol. 3, pp. 38-51, 1985.
- [6] Y. Nino, "Particle motion in the near bed region of a turbulent open channel flow: implications for bedload transport by saltation and sediment entrainment into suspension," Doctoral dissertation, University of Illinois at Urbana-Champaign, 1995.
- [7] H. Y. Lee, J. Y. You, Y. T. Lin, "Continuous saltating process of multiple sediment particles," *Journal of hydraulic engineering*, Vol.128, No.4, pp. 443-450, 2002.
- [8] N. Lukerchenko, Z. Chara, P. Vlasak, "2D Numerical model of particle–bed collision in fluid-particle flows over bed," *Journal of Hydraulic Research*, Vol.44, No.1, pp. 70-78, 2006.
- [9] A. Nasrollahi, S.A.A. Salehi Neyshabouri, G. Ahmadi, M.M. Namin, "Numerical Simulation of Particle Saltation Process," *Particulate Science and Technology*, Vol.26, No.6, pp. 529-550, 2008.
- [10] N. Lukerchenko, S. Piatsevich, Z. Chara, P. Vlasak, Z. Chára, P. Vlasák, "3D numerical model of the spherical particle saltation in a channel with a rough fixed bed," *Journal of Hydrology and Hydromechanics*, Vol.57, No.2, pp. 100-112, 2009.
- [11] R. J. Bialik, "Particle–particle collision in Lagrangian modelling of saltating grains," *Journal of Hydraulic Research*, Vol.49, No.1, pp. 23-31, 2011.

- [12] W. Czernuszenko, R. J. Bialik, "Some Properties of Lagrangian Modeling of Saltating Grains Over Movable Bed," In *Experimental and Computational Solutions of Hydraulic Problems, GeoPlanet: Earth and Planetary Sciences*, pp. 273-283, 2013.
- [13] M. Jafari, Z. Mansoori, M. S. Avval, G. Ahmadi, A. Ebadi, "Modeling and numerical investigation of erosion rate for turbulent two-phase gas-solid flow in horizontal pipes," *Powder Technology*, Vol.267, 362-370, 2014.
- [14] M. Jafari, Z. Mansoori, M. S. Avval, G. Ahmadi, "The effects of wall roughness on erosion rate in gas-solid turbulent annular pipe flow," *Powder Technology*, 2014.
- [15] R. Barati, S. A. A. Salehi Neyshabouri, G. Ahmadi, "Numerical simulation of the sediment transport in the saltation regime," *River Flow 2014 - the 7th International Conference on Fluvial Hydraulics – at EPFL, Lausanne, Switzerland*, 2014.
- [16] R. Barati, S. A. A. Salehi Neyshabouri, G. Ahmadi, "Development of a 3D Lagrangian model for numerical simulation of initiation of motion of sediment particles" *The 11th International Conference on Coasts, Ports and Marine Structures (ICOPMAS 2014)*, Tehran, Iran, 24-26, pp. 215–218, 2014.
- [17] A. E. Gonzalez, "Numerical modeling of sediment transport near the bed using a two-phase flow approach," *University of California, Davis*, 2008.
- [18] M. R. Maxey, J. J. Riley, "Equation of motion for a small rigid sphere in a nonuniform flow," *Physics of Fluids*, Vol. 26, pp. 883-889, 1983.
- [19] P. L., Wiberg, J. D. Smith, "A theoretical model for saltating grains in water," *Journal of Geophysical Research: Oceans (1978–2012)*, Vol. 90(C4), pp. 7341-7354, 1985.
- [20] R. Barati, S. A. A. Salehi Neyshabouri, G. Ahmadi, "Sphere Drag Revisited Using Shuffled Complex Evolution algorithm," *River Flow 2014 - the 7th International Conference on Fluvial Hydraulics – at EPFL, Lausanne, Switzerland*, 2014.
- [21] R. Barati, S. A. A. Salehi Neyshabouri, G. Ahmadi, "Development of empirical models with high accuracy for estimation of drag coefficient of flow around a smooth sphere: An evolutionary approach," *Powder Technology*, Vol. 257, pp. 11-19, 2014.
- [22] A., Yeganeh-Bakhtiary, B., Shabani, H., Gotoh, S. S. Wang, "A three-dimensional distinct element model for bed-load transport," *Journal of Hydraulic Research*, Vol.47, No.2, pp. 203-212, 2009.
- [23] N. Lukerchcenko, J. Dolansky, P. Vlasak, "Basset force in numerical models of saltation," *J. Hydrol. Hydromech.*, Vol.60, No.4, 277–287, 2012.
- [24] R. J. Bialik, "Numerical study of near-bed turbulence structures influence on the initiation of saltating grains movement," *J. Hydrol. Hydromech.*, Vol.61, No.3, pp. 202–207, 2013.